

## Atomic Hydrogen Adsorbate Structures on Graphene

Richard Balog, Bjarke Jørgensen, Justin Wells, Erik Lægsgaard, Philip Hofmann,<sup>†</sup>  
Flemming Besenbacher, and Liv Hornekær\*

Department of Physics and Astronomy and Interdisciplinary Nanoscience Center (iNANO),  
Aarhus University, Denmark

Received April 5, 2009; E-mail: liv@phys.au.dk

Graphene, a single atomic layer of graphite, has recently attracted considerable attention due to its remarkable electronic and structural properties and its possible application in the emerging area of graphene based electronic devices<sup>1</sup> and as a hydrogen storage material.<sup>2</sup> The charge carriers in graphene behave like massless Dirac fermions, and graphene exhibits ballistic charge transport properties which make it an ideal material for electronic device and circuit fabrication.<sup>3</sup> However, graphene is a semimetal, a zero band gap semiconductor, and for graphene to become a versatile electronic device material it is mandatory to find means to open up the band gap and tune the size of the band gap opening. Several strategies have been suggested to engineer such a band gap opening in graphene in a controlled way. Some of these are based on the ability to control the geometry of graphene nanoribbons<sup>4</sup> or by use of graphene–substrate interactions,<sup>5</sup> while others are based on chemical reactions of atomic hydrogen with the graphene layer.<sup>2,6–9</sup>

To efficiently utilize such chemical doping with H atoms, knowledge of the binding properties of hydrogen atoms on the graphene surface are needed. We present scanning tunneling microscopy (STM) studies which reveal the adsorbate structures of atomic hydrogen on the basal plane of graphene on a SiC substrate. At low hydrogen coverage the formation of hydrogen dimer structures is revealed, while at higher coverage larger disordered hydrogen clusters are observed. Dimer formation is observed to occur preferentially on protruding/high tunneling probability areas of the graphene layer which is modulated by the underlying  $6 \times 6$  reconstruction of the SiC (0001)-(1  $\times$  1) surface. Hydrogenation is observed to be reversible by thermal annealing.

To investigate the adsorption of atomic hydrogen on graphene, a graphene sample was prepared on a SiC (0001)-(1  $\times$  1) surface (see Supporting Information for further details) and exposed to a 1600 K D-atom beam for 5 s at a flux of  $10^{12}$ – $10^{13}$  atoms/cm<sup>2</sup> s. Figure 1a displays an STM image of the graphene sample after hydrogen exposure. A number of bright protrusions are observed which are attributed to hydrogen adsorbates. The detailed analysis of these structures reveals different hydrogen configurations: ortho-dimers (structure A in inset in Figure 1a), para-dimers (structure B in inset in Figure 1a), and various extended dimer structures and monomers, marked in Figure 1a as A, B, C, and D, respectively. The hydrogen adsorbates have been identified according to their size and shape based on a detailed and thorough comparison with the experimentally observed hydrogen dimer structures on graphite<sup>10</sup> and with simulated STM images of hydrogen on graphene based on Density Functional Theory (DFT) calculations using the simple Tersoff and Haman model for the tunnel current, which represent the local density of state (LDOS) at the Fermi level.<sup>10</sup> The DFT calculations reveal that the ortho- and para-dimers are energetically

the most stable configurations on the basal plane of both graphene and graphite.<sup>9–11</sup> It has been suggested that dimer formation proceeds via preferential binding into dimer structures during hydrogen exposure, since the barriers and the sticking probability to bind into dimers are lower compared to these for hydrogen adsorption into monomers.<sup>12,13</sup> We do not observe any significant differences between hydrogen dimers on graphite and those on graphene. Furthermore, data indicate the same route for dimer formation on both substrates. On the other hand, no monomers have been reported on graphite surfaces at room temperature and very low coverage, which is in contrast to the findings for hydrogen on graphene. The observation of monomers tentatively suggests that atomic hydrogen is more strongly bound to epitaxial graphene than to graphite, thus increasing its survival time at the surface and/or that the barrier to adsorb into a monomer site is reduced on graphene compared to graphite.

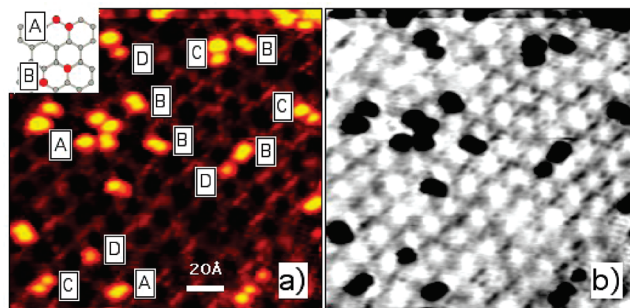


**Figure 1.** (a) Scanning tunneling microscopy image of hydrogenated graphene. The bright protrusions visible in the image are atomic hydrogen adsorbate structures identified as A = ortho-dimers, B = para-dimers, C = elongated dimers, D = monomers (imaging parameters:  $V_t = -0.245$  V,  $I_t = -0.26$  nA). Inset in (a): Schematic of the A ortho- and B para-dimer configuration on the graphene lattice. (b) Same image as in (a) with inverted color scheme, giving emphasis to preferential hydrogen adsorption along the  $6 \times 6$  modulation on the SiC (0001)-(1  $\times$  1) surface. Hydrogen dose at  $T_{\text{beam}} = 1600$  K,  $t = 5$  s,  $F = 10^{12}$ – $10^{13}$  atoms/cm<sup>2</sup> s.

Remarkably we find that a preference exists for H adsorption on certain well-defined areas of the graphene surface layer. As depicted in Figure 1b, we have observed that, at low coverage, the majority of hydrogen adsorbates follow the  $6 \times 6$  modulation of the surface. To emphasize the effect, the STM image is inverted in color. Hydrogen adsorbates, the dark spots, are seen to be preferentially located on the gray areas of the surface. One possible explanation is that this effect originates from buckling of the graphene layer.<sup>14</sup> Both calculations and experiments on hydrogenation of different forms of graphene, like fullerenes<sup>15</sup> or single wall carbon nanotubes (CNTs)<sup>16,17</sup> show that geometrical deformation plays a key role in determining the chemical reactivity with hydrogen. For example, the curvature of CNTs strongly influences

<sup>†</sup> Institute for Storage Ring Facilities and Interdisciplinary Nanoscience Center (iNANO), Aarhus University, Denmark.

both the barrier for sticking and the binding energy of chemisorbed hydrogen. While the barrier for hydrogen sticking decreases for high surface curvature, the binding energy increases.<sup>16</sup> The decrease in sticking barrier can be explained by the fact that H chemisorption is accompanied by hybridization changes of the carbon from  $sp^2$  to  $sp^3$ , resulting in a relaxation of the carbon atom toward the hydrogen adsorbate. This reaction induced relaxation costs elastic potential energy, and this cost is reduced on surfaces, which are already deformed in the proper direction. Hence, convex areas can then be viewed as precursors for carbon puckering and are therefore energetically favorable binding sites.<sup>7</sup> If we assume that the topological surface corrugation follows the  $6 \times 6$  modulation,<sup>14</sup> we may expect the H atoms to bind preferentially onto the apexes of the modulated graphene surface, as observed. An alternative possibility is that the enhanced reactivity has an electronic origin.<sup>18</sup>

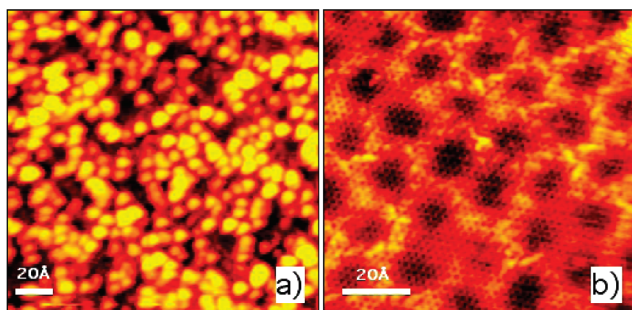


**Figure 2.** (a) STM image of the graphene surface after extended hydrogen exposure. The bright protrusions in the image are identified as atomic hydrogen clusters (imaging parameters:  $V_t = -0.36$  V,  $I_t = -0.32$  nA). Hydrogen dose at  $T = 1600$  K,  $t = 90$  s,  $F = 10^{12}$ – $10^{13}$  atoms/cm<sup>2</sup> s. (b) Large graphene area recovered from hydrogenation by annealing to 800 °C (imaging parameters:  $V_t = -0.38$  V,  $I_t = -0.410$  nA).

In Figure 2a, a hydrogen covered graphene surface is displayed. The sample was exposed to a 90 s dose of hydrogen atoms from a beam at 1600 K and a flux of  $10^{12}$ – $10^{13}$  atoms/cm<sup>2</sup> s. The sample was kept at room temperature during the hydrogen deposition and subsequent STM measurement. Hydrogen adsorbates are visible as the bright protrusions covering the entire surface. From the recorded STM images at this coverage no indication for preferential adsorption of hydrogen on any specific parts of the graphene surface is revealed. The large bright protrusions visible in the image in Figure 2a indicate that hydrogen tends to form larger hydrogen clusters at increased coverage similar to those observed for hydrogen adsorbates on graphite.<sup>12</sup> For these large bright protrusions the underlying hydrogen adsorbate atomic scale structure could not be determined. Therefore, we are unable to estimate the hydrogen coverage from the STM data. However, temperature programmed desorption (TPD) and X-ray photoelectron spectroscopy (XPS) measurements of hydrogen adsorbates on graphite show a saturation coverage of 0.4 ML.<sup>19</sup> Since the high coverage structures observed in STM for hydrogen on graphene are similar to those observed for hydrogen on graphite, we tentatively assume a similar saturation coverage. A constraint on the coverage is imposed by the two competitive processes: H adsorption and Eley–Rideal abstraction. The latter process is very efficient and leads to gas phase H<sub>2</sub> with a cross section ranging from  $17 \text{ \AA}^2$  (low coverage) to  $4 \text{ \AA}^2$  (high coverage).<sup>20</sup> In addition, it has been predicted theoretically that complete, one side hydrogenation of graphene is thermodynamically unstable.<sup>2,8</sup> We have observed that the STM tip tunneling can induce hydrogen desorption, which implies that the hydrogen is bound fairly weakly to the graphene surface. The sample is recovered to its original state by annealing the substrate to 800 °C. Figure 2b

displays an STM image of the sample after many hydrogen deposition–annealing cycles. No distinguished damage of the graphene layers could be observed.

In conclusion, we have revealed the local adsorbate structures of single sided hydrogenated graphene at both low and high hydrogen coverage. At low coverage the formation of hydrogen dimers occurs preferentially on the protruding areas in the STM topographs of the graphene–SiC surface, while at higher coverage random adsorption into larger hydrogen clusters is observed. Thermal annealing experiments in combination with STM indicate that hydrogenation is reversible. Preferential adsorption of atomic hydrogen onto protruding areas on the surface, as well as the ability to form nanopatterns via tip-induced desorption of hydrogen, opens up the possibility of electronic and chemical functionalization of graphene surfaces via hydrogenation.

**Acknowledgment.** L.H. acknowledges financial support from the Danish National Science Council and through ERC starting grant 208322 HPAH.

**Note Added after ASAP Publication.** The version of this paper published on May 29, 2009, had errors in reference 8. The corrected version was published on June 4, 2009.

**Supporting Information Available:** Details of the experimental setup and methods and graphene sample preparation and characterization. This material is available free of charge via the Internet at <http://pubs.acs.org>.

## References

- (1) Geim, A.; Novoselov, K. *Nat. Mater.* **2007**, *6*, p 183–191.
- (2) Sofo, J. O.; Chaudhari, A. S.; Barber, G. D. *Phys. Rev. B* **2007**, *75*, p 153401.
- (3) (a) Novoselov, K.; Geim, A.; Morozov, S.; Jiang, D.; Katsnelson, M.; Grigorieva, I.; Dubonos, S.; Firsov, A. *Nature* **2005**, *438*, 197. (b) Hass, J.; Feng, R.; Li, T.; Li, X.; Zong, Z.; de Heer, W. A.; First, P. N.; Conrad, E. H.; Jeffrey, C. A.; Berger, C. *Appl. Phys. Lett.* **2006**, *89*, 143106.
- (4) Berger, C. *Science* **2006**, *312*, p 1191–1196.
- (5) Giovannetti, G.; Khomyakov, P. A.; Brocks, G.; Kelly, P. J.; van den Brink, J. *Phys. Rev. B* **2007**, *76*, 073103.
- (6) Chernozatonskii, L.; Sorokin, P.; Belova, E.; Brüning, J.; Fedorov, A. *JETP Lett.* **2007**, *85*, 77–81.
- (7) (a) Elias, D.; Nair, R.; Mohiuddin, T.; Morozov, S.; Blake, P.; Halsall, M.; Ferrari, A.; Boukhvalov, D.; Katsnelson, M.; Geim, A.; Novoselov, K. *Science* **2009**, *323*, 610–613. (b) Ryu, S.; Han, M. Y.; Maultzsch, J.; Heinz, T. F.; Kim, P.; Steigerwald, M. L.; Brus, L. E. *Nano Lett.* **2008**, *8*, 4597–4602.
- (8) Boukhvalov, D. W.; Katsnelson, M. I.; Lichtenstein, A. I. *Phys. Rev. B* **2008**, *77*, 035427.
- (9) Casolo, S.; Lovvik, O. M.; Martinazzo, R.; Tantardini, G. F. *J. Chem. Phys.* **2009**, *130*, 054704.
- (10) Hornekaer, L.; Slijivancanin, Z.; Xu, W.; Otero, R.; Rauls, E.; Stensgaard, I.; Laegsgaard, E.; Hammer, B.; Besenbacher, F. *Phys. Rev. Lett.* **2006**, *96*, 156104.
- (11) Ferro, Y.; Teillet-Billy, D.; Rougeau, N.; Sidis, V.; Morisset, S.; Allouche, A. *Phys. Rev. B* **2008**, *78*, 8.
- (12) Hornekaer, L.; Rauls, E.; Xu, W.; Slijivancanin, Z.; Otero, R.; Stensgaard, I.; Laegsgaard, E.; Hammer, B.; Besenbacher, F. *Phys. Rev. Lett.* **2006**, *97*, 186102.
- (13) (a) Rougeau, N.; Teillet-Billy, D.; Sidis, V. *Chem. Phys. Lett.* **2006**, *431*, 135–138. (b) Cuppen, H.; Hornekaer, L. *J. Chem. Phys.* **2008**, *128*, 174707. (c) Kerwin, J.; Jackson, B. *J. Chem. Phys.* **2008**, *128*, 084702.
- (14) (a) Varchon, F.; Mallet, P.; Veuillen, J.; Magaud, L. *Phys. Rev. B* **2008**, *77*, 235412. (b) Rutter, G.; Guisinger, N.; Crain, J.; Jarvis, E.; Stiles, M.; Li, T.; First, P.; Stroscio, J. *Phys. Rev. B* **2007**, *76*, 6.
- (15) Ruffieux, P.; Groning, O.; Bielmann, M.; Mauron, P.; Schlapbach, L.; Groning, P. *Phys. Rev. B* **2002**, *66*, 245416.
- (16) (a) Park, S.; Srivastava, D.; Cho, K. *Nano Lett.* **2003**, *3*, 1273–1277. (b) Zhou, B.; Guo, W.; Tang, C. *Nanotechnol.* **2008**, *19*, 075707.
- (17) (a) Zhang, G. Y.; Qi, P. F.; Wang, X. R.; Lu, Y. R.; Mann, D.; Li, X. L.; Dai, H. *J. Am. Chem. Soc.* **2006**, *128*, 6026–6027. (b) Nikitin, A.; Zhang, Z.; Nilsson, A. *Nano Lett.* **2009**, *9*, 1301–1306.
- (18) Riedl, C.; Starke, U.; Bernhardt, J.; Franke, M.; Heinz, K. *Phys. Rev. B* **2007**, *76*, 245406.
- (19) (a) Zecho, T.; Guttler, A.; Sha, X. W.; Jackson, B.; Kuppers, J. *J. Chem. Phys.* **2002**, *117*, 8486–8492. (b) Nikitin, A.; Naslund, L.; Zhang, Z.; Nilsson, A. *Surf. Sci.* **2008**, *602*, 2575–2580.
- (20) Zecho, T.; Guttler, A.; Sha, X. W.; Lemoine, D.; Jackson, B.; Kuppers, J. *Chem. Phys. Lett.* **2002**, *366*, 188–195.

JA902714H